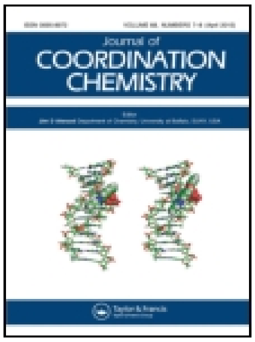

Journal of Coordination Chemistry

ISSN: 0095-8972 (Print) 1029-0389 (Online) Journal homepage: http://www.tandfonline.com/loi/gcoo20

3D Heterometallic 3d–4f coordination polymers based on organodisulfonate ligand with isonicotinic acid as a co-ligand: synthesis, crystal structures, photoluminescent and magnetic properties

Wei-Ping Xie, Li-Ping Lu, Shao-Bin Feng, Xing-Rui Ran, Jin-Ying Gao, Chu-Jun Chen, Shan-Tang Yue & Yue-Peng Cai

To cite this article: Wei-Ping Xie, Li-Ping Lu, Shao-Bin Feng, Xing-Rui Ran, Jin-Ying Gao, Chu-Jun Chen, Shan-Tang Yue & Yue-Peng Cai (2015) 3D Heterometallic 3d–4f coordination polymers based on organodisulfonate ligand with isonicotinic acid as a co-ligand: synthesis, crystal structures, photoluminescent and magnetic properties, Journal of Coordination Chemistry, 68:10, 1776-1787, DOI: 10.1080/00958972.2015.1027696

To link to this article: http://dx.doi.org/10.1080/00958972.2015.1027696

Journal of Coordination Chemistry, 2015
Vol. 68, No. 10, 1776–1787, http://dx.doi.org/10.1080/00958972.2015.1027696

3D Heterometallic 3d–4f coordination polymers based on organodisulfonate ligand with isonicotinic acid as a co-ligand: synthesis, crystal structures, photoluminescent and magnetic properties

WEI-PING XIE, LI-PING LU, SHAO-BIN FENG, XING-RUI RAN, JIN-YING GAO, CHU-JUN CHEN, SHAN-TANG YUE* and YUE-PENG CAI

School of Chemistry and Environment, South China Normal University, Guangzhou, PR China

(*Received 12 November 2013; accepted 15 January 2015*)

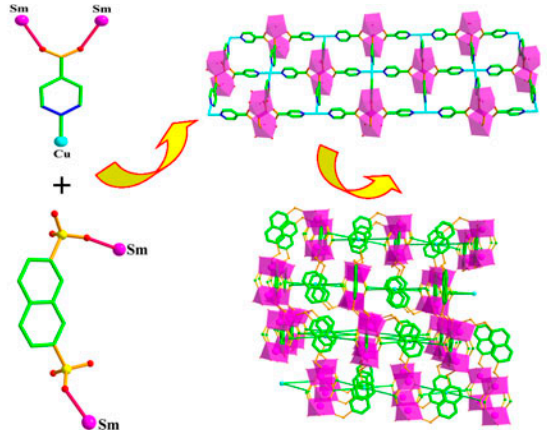

The hydrothermal reaction of rare earth nitrates, CuCN, 2,7-naphthalenedisulfonate (2,7-nds), and isonicotinic acid (Hina) affords a new family of 3-D heterometallic 3d–4f coordination polymers, $[Ln_2Cu(2,7\text{-nds})_2(ina)_4(H_2O)_4]\cdot 4H_2O$ (Ln = Nd (**1**), Sm (**2**), Eu (**3**), Gd (**4**); 2,7-nds = 2,7-naphthalenedisulfonate, Hina = isonicotinic acid). Complexes **1–4** are structurally characterized by single crystal X-ray diffraction, elemental analysis, FT-IR spectroscopy (IR), powder X-ray diffraction, and thermogravimetric analyses. X-ray crystal structure analyses reveal that **1–4** are isomorphous with dinuclear subunit $[Sm_2(ina)_4]$ binding Cu ions to generate 2-D networks. Such 2-D networks are pillared by linking 2,7-nds ligands to result in the 3-D layer-pillared Ln(III)–Cu(II) coordination architectures. The valence of Cu salts changed in the reaction. In addition, the luminescence properties of **1–3** and the magnetic properties of **3** and **4** have also been investigated.

Keywords: Hydrothermal synthesis; Heterometallic; 2,7-Naphthalenedisulfonate; Luminescence; Magnetism

---

*Corresponding author. Email: yuesht@scnu.edu.cn

1. Introduction

Synthesis of metal–organic frameworks (MOFs) based on arenedisulfonate ligands is one of the hottest fields in supramolecular chemistry and crystal engineering [1–3], due to the flexible coordination modes of SO_3^- groups which contribute to novel structural architectures and topologies [4–6], and their potential applications in catalysis [7], absorption [8, 9], magnetism [10], optics [11], and single-crystal-to-single-crystal conversion [12]. However, a careful review of the literature suggests that among the various structures of metal organosulfonates, most of the work has been for main group, transition metal, or lanthanide ion coordination frameworks based on arenedisulfonate [13–15]; lanthanide-transition heterometallic compounds are still limited [16]. Furthermore, there is rare report on d–f heterometallic compounds synthesized using 2,7-naphthalenedisulfonate (2,7-nds). We have reported Cu–Ln and Ag–Ln heterometallic compounds using 2,6-naphthalenedisulfonate (2,6-nds), 2,7-naphthalenedisulfonate (2,7-nds), and isonicotinic acid as a second ligand. Because the two $–SO_3$ locate in different places of the naphthalene ring in 2,6-nds and 2,7-nds, and the different coordination mode of Cu, which prefers two- or four-coordinate, and Ag which prefers two- or three-coordinate, the 3-D structures of these complexes have their own characteristics [17, 18]. Heterometallic coordination polymers not only possess fascinating topologies and intriguing architectures [19, 20], but also have a wide range of applications in magnetism [21, 22], luminescence [23, 24], sorption [25, 26], and bimetallic catalysis [27, 28]. Yet, the preparation of lanthanide-transition heterometallic coordination frameworks is still a challenge for the sulfonate family since organosulfonates are regarded as weak bonding ligands [29–31] and lanthanide and transition metal ions have a competition during coordination to ligands. Fortunately, lanthanide and transition metal ions have different affinities for N and O donors according to the hard–soft acid/base classification [32], which provides the impetus to construct d–f heteronuclear arenedisulfonate MOFs by introducing secondary ligands.

In this context, we use isonicotinic acid as the auxiliary ligand due to the following reasons: (i) isonicotinic acid contains both N and O donors, so that it can greatly increase the possibility of obtaining d–f heterometallic coordination polymers; (ii) it is a rigid and linear ligand, which plays an important role in constructing high-dimensional MOFs [33, 34]. Following this strategy, a new family of 3-D heterometallic 3d–4f coordination polymers, $[Ln_2Cu(2,7\text{-nds})_2(ina)_4(H_2O)_4]\cdot 4H_2O$ (Ln = Nd (**1**), Sm (**2**), Eu (**3**), Gd (**4**); 2,7-nds = 2,7-naphthalenedisulfonate, Hina = isonicotinic acid), have been synthesized under hydrothermal conditions. Their structures have been determined by single-crystal X-ray diffraction analyses and further characterized by infrared spectra (IR), elemental analyses (EA), powder X-ray diffraction (PXRD), and thermogravimetric analyses (TGA). Bu *et al.* reported the first single lanthanide-2,7-nds (Ln = Eu, Gd, Tb) supramolecular structure and Ng *et al.* obtained the single Ba-2,7-nds and Sr-2,7-nds complexes with 2-D structures [14, 35]. Thus, **1–4** are the first examples of Ln(III)–Cu(II) layer-pillared 3d–4f heterometallic compounds based on 2,7-nds and the two Ln ions are linked by four carboxylate groups in a classic paddle-wheel fashion similar to the units of Ln(III)-4-Hcba (4-Hcba = 4-cyanobenzoic acid; Ln = Pr, Nd, Sm, Eu, Gd, Dy) links reported by Huang [36] and Ln(III)-bpdc (bpdc = 2,2′-bipyridine-3,3′-dicarboxylate; Ln = Nd, Eu, Tb) links by Guo and Guo [37], with carboxylate ligands as linear linkers that form 2-D layers. However, these two examples generate 3-D structures only by the π–π interaction between ligands. The complexes we report in this article generate 3-D structures by 2,7-naphthalenedisulfonate (2,7-nds) coordinating at both sides of Ln_2

paddle-wheel units to bridge the layers vertically. In **1–4** structures, 2,7-nds ligands and ina–Cu–ina chains connected two square antiprisms to build the 3-D structure. In addition, the magnetic properties of **3** and **4** have also been investigated.

2. Experimental

2.1. *Materials and physical measurements*

All chemicals were obtained from commercial sources and used without purification. EA for C, H, and N were performed on a Perkin-Elmer 2400 elemental analyzer. The FT-IR samples were prepared as KBr pellets, and spectra were obtained from 4000 to 400 cm^{-1} on a Nicolet 5DX spectrometer. TGA were carried out on a Perkin-Elmer TGA7 thermogravimetric analyzer with the heating rate of 10 °C min^{-1} under dry air. X-ray powder diffraction measurements were measured on an X-pert diffractometer or Rigaku D/M-2200T automated diffractometer for Cu Kα radiation (λ = 1.54056 Å) with a scan speed of 4° min^{-1} in 2θ range of 5–50°. The luminescence spectra for the solid state were recorded at room temperature on an Edinburgh FLS920 with a Xe900 xenon arc lamp as the exciting light source. Magnetic susceptibility data were collected from polycrystalline samples at an external field of 1000 Oe on a MPMS XL-7 magnetometer (quantum design) from 2 to 300 K. The output data were corrected for diamagnetism of the sample holder and calculated for the polymers by Pascal constants.

2.2. *X-ray crystallography*

Single crystals of **1–4** were mounted on a Bruker Apex II CCD diffractometer operating at 50 kV and 30 mA using Mo Kα radiation (λ = 0.71073 Å) at room temperature. Data collection and reduction were performed using APEX II software. Multiscan absorption corrections were applied for all the data-sets using the APEX II program. All four structures were solved by direct methods and refined by full-matrix least squares fitting on F^2 using the SHELXTL program package [38, 39]. All non-hydrogen atoms were refined anisotropically. Hydrogens attached to carbon were located at geometrically idealized positions and refined using a riding model. Hydrogens on water were located from difference Fourier maps and were also refined using a riding model. Details of the crystal parameters, data collections, and refinements for **1–4** are summarized in table 1. Selected bond lengths and angles are listed in table S1 (see online supplemental material at http://dx.doi.org/10.1080/00958972.2015.1027696).

2.3. *Synthesis of 1–4*

A mixture of 2,7-naphthalenedisulfonate sodium salt (0.1661 g, 0.5 mmol), isonicotinic acid (0.127 g, 1.0 mmol), $Nd(NO_3)_3\cdot 6H_2O$ for **1** (0.1318 g, 0.3 mmol), $Sm(NO_3)_3\cdot 6H_2O$ for **2** (0.1333 g, 0.3 mmol), $Eu(NO_3)_3\cdot 6H_2O$ for **3** (0.1338 g, 0.3 mmol), $Gd(NO_3)_3\cdot 6H_2O$ for **4** (0.1353 g, 0.3 mmol), and CuCN (0.0276 g, 0.3 mmol) were dissolved in 8 mL of H_2O, then heated to 160 °C for 72 h in a 23 mL Teflon-lined stainless steel autoclave. After cooling to room temperature at 5 °C h^{-1}, blue block crystals suitable for X-ray diffraction analysis were collected manually, washed with distilled water several times, and dried in air.

Table 1. Crystal data and structure refinement parameters of **1–4**.

Complex	**1**	**2**	**3**	**4**
Empirical formula	$C_{44}H_{44}Nd_2CuN_4O_{28}S_4$	$C_{44}H_{44}Sm_2CuN_4O_{28}S_4$	$C_{44}H_{44}Eu_2CuN_4O_{28}S_4$	$C_{44}H_{44}Gd_2CuN_4O_{28}S_4$
Formula weight	1557.14	1569.38	1572.60	1583.16
T (K)	298(2)	298(2)	298(2)	298(2)
Crystal system	Tetragonal	Tetragonal	Tetragonal	Tetragonal
Space group	$P4_32_12$	$P4_32_12$	$P4_32_12$	$P4_32_12$
a (Å)	12.6877(18)	12.666(2)	12.657(3)	12.6266(13)
b (Å)	12.6877(18)	12.666(2)	12.657(3)	12.6266(13)
c (Å)	33.928(5)	33.841(6)	33.766(8)	33.793(3)
α (°)	90	90	90	90
β (°)	90	90	90	90
γ (°)	90	90	90	90
V (Å^3)	5461.7(17)	5429(2)	5409(3)	5387.7(12)
Z	4	4	4	4
D_{Calcd} (g cm^{-3})	1.894	1.920	1.931	1.952
μ (mm^{-1})	2.507	2.773	2.931	3.076
F (0 0 0)	3092.0	3108.0	3116.0	3124.0
GOF	1.107	1.065	1.139	1.258
R_1 [$I > \sigma(I)$]^a	$R_1 = 0.0422$	$R_1 = 0.0458$	$R_1 = 0.0813$	$R_1 = 0.0719$
wR_2 (all data)^b	$wR_2 = 0.0933$	$wR_2 = 0.1030$	$wR_2 = 0.1802$	$wR_2 = 0.1624$
Data/restraints/parameters	4811/0/366	5338/9/384	6296/25/368	4967/38/371

$^aR_1 = \sum \|F_o| - |F_c\| / \sum |F_o|$.

$^bwR_2 = \{\sum[w(F_o^2 - F_c^2)^2] / \sum(F_o^2)^2]\}^{1/2}$.

2.3.1. {$Nd_2Cu(2,7\text{-nds})_2(ina)_4(H_2O)_4] \cdot 4H_2O$} (1). 0.1288 g, yield 55% based on Nd. Anal. Calcd for $C_{44}H_{44}Nd_2CuN_4O_{28}S_4$: C, 33.91; H, 2.83; N, 3.60%. Found: C, 33.89; H, 2.80; N, 3.58%. IR data (KBr, cm^{-1}): 3349 m, 1655 s, 1555 w, 1396 s, 1233 m, 1171 s, 1120 m, 1034 s, 777 m, 707 m, 690 s.

2.3.2. {$Sm_2Cu(2,7\text{-nds})_2(ina)_4(H_2O)_4] \cdot 4H_2O$} (2). 0.1248 g, yield 53% based on Sm. Anal. Calcd for $C_{44}H_{44}Sm_2CuN_4O_{28}S_4$: C, 33.64; H, 2.80; N, 3.57%. Found: C, 33.62; H, 2.79; N, 3.55%. IR data (KBr, cm^{-1}): 3401 s, 1657 s, 1558 w, 1399 s, 1234 m, 1179 s, 1119 m, 1031 s, 779 m, 710 m, 693 s.

2.3.3. {$Eu_2Cu(2,7\text{-nds})_2(ina)_4(H_2O)_4] \cdot 4H_2O$} (3). 0.1109 g, yield 47% based on Eu. Anal. Calcd for $C_{44}H_{44}Eu_2CuN_4O_{28}S_4$: C, 33.57; H, 2.79; N, 3.56%. Found: C, 33.55; H, 2.76; N, 3.54%. IR data (KBr, cm^{-1}): 3307 m, 1660 s, 1556 w, 1400 s, 1235 m, 1172 s, 1118 m, 1033 s, 778 m, 706 m, 691 s.

2.3.4. {$Gd_2Cu(2,7\text{-nds})_2(ina)_4(H_2O)_4] \cdot 4H_2O$} (4). 0.1069 g, yield 45% based on Gd. Anal. Calcd for $C_{44}H_{44}Gd_2CuN_4O_{28}S_4$: C, 33.31; H, 2.78; N, 3.53%. Found: C, 33.29; H, 2.76; N, 3.51%. IR data (KBr, cm^{-1}): 3433 s, 1661 s, 1557 w, 1401 s, 1232 m, 1175 s, 1114 m, 1035 s, 776 m, 707 m, 691 m.

3. Results and discussion

3.1. *Crystal structure descriptions*

Complexes **1–4** are isomorphous, established by single-crystal X-ray crystallography; hence **2** is used as a representative example to describe here. Complex **2** crystallizes in the

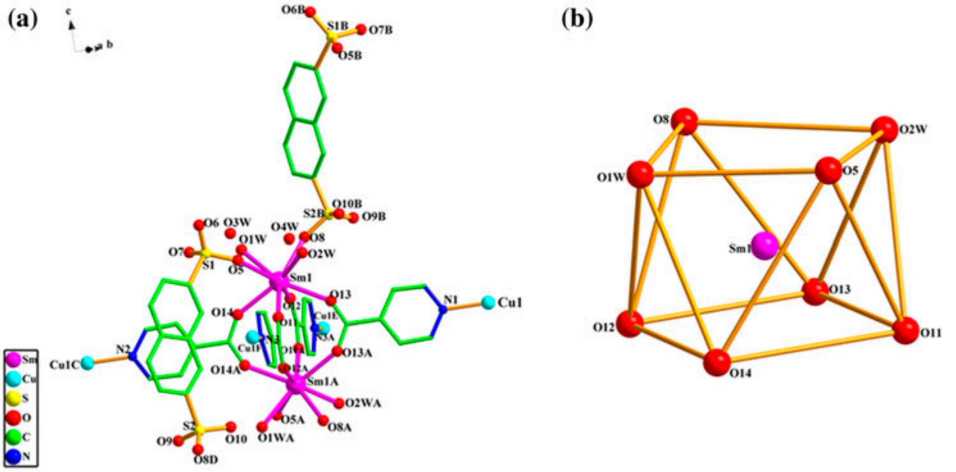

Figure 1. (a) Coordination environment of Sm and Cu in **2**. The thermal ellipsoids are drawn at 50% probability. All hydrogens are omitted for clarity. Symmetry codes: (A) 1 + *x*, −1 + *y*, −*z*; (B) 1.5 − *x*, −0.5 + *y*, 0.25 + *z*; (C) −1 + *x*, −1 + *y*, *z*; (D) 0.5 + *x*, 1.5 − *y*, −0.25 + *z*; (E) −1 + *x*, *y*, *z*; (F) *x*, −1 + *y*, *z*. (b) Coordination geometry of the Sm(III) ion.

tetragonal space group $P4_32_12$. As shown in figure 1(a), the asymmetric unit of **2** contains one Sm(III) ion, one-half Cu(II) ion, one independent 2,7-nds ligand, one independent ina ligand, two one-half ina ligands, and two coordinated and two lattice water molecules. Two Sm(III) ions are connected by four carboxylic groups adopting μ_2-$\eta^1 : \eta^1$ coordination to form a dimer. Each Sm(III) is coordinated by eight oxygens, in which four oxygens belong to four ina ligands, two oxygens belong to two different 2,7-nds ligands, and two oxygens are waters. The coordination sphere of each Sm(III) can be described as a distorted square antiprism [figure 1(b)], and the dihedral angle between the upper and lower planes is about 0.578(153)°. The two planes of square antiprism structure are O1 W, O2 W, O5, O8 and O11, O12, O13, O14, respectively [40]. There are three different types of oxygens coordinated to Ln ions, so that the Sm1–O bond lengths are 2.4388(18) Å and 2.417(3) Å for O1 W and O2 W from water molecules, 2.575(3) Å and 2.444(3) Å for O5 and O8 atoms from 2,7-nds ligands, 2.371(3) to 2.426(3) Å for O11, O12, O13, and O14 from ina ligands, comparable to the Ln–O bond distances of $LnCu(nds)(ina)_2H_2O$ [nds = 2,6-nds; Ln = Eu (1), Ce (2), Er (3), Gd (4), Sm (5), Tb(6), Dy(7)] reported by our group [17]. The O–Sm1–O bond angles are 67.42(17)°–148.0(2)°. It is not appropriate to use the terms *syn* and *anti* to describe the coordination mode of metal arenedisulfonate, so the torsion angles of C–S–O–Sm are used [41, 42]. The torsion angles of C(9)–S(1)–O(5)–Sm(1) and C(3)–S(2)–O(8)–Sm(1) are 98.359(551)° and 130.319(539)°, respectively. The Cu(II) has a plane quadrilateral coordination geometry and is coordinated by four nitrogens from four ina ligands. Although the starting material is Cu(I) salts, the Cu center in the final product is bivalent, attributed to oxidation occurring under the hydrothermal conditions [43]. Based on search of the Cambridge Structural Database, Cu(II) ions prefer to adopt four- or six-coordinate mode, while Cu(I) ions prefer to adopt a two- or three-coordinate mode [17, 44–47], which further demonstrates that the Cu(I) has been oxidized. The Cu–N bond lengths are 2.014(9)– 2.027(6) Å, which are similar to those found in related Cu(II) compounds [43, 44]. The vertical angles of this plane are quadrilateral, the N–Cu–N bond angles are 90.00 (18)°. For **1–4**, all the lanthanide ions are eight-coordinate, and the Nd–O (**1**), Sm–O (**2**), Eu–O (**3**), Gd–O (**4**) distances decrease gradually as listed in table S1 because of the lanthanide contraction [45–51].

In the structure of **2**, the ina ligands have one coordination mode: the nitrogen coordinates to Cu center and the carboxylate connects to two Sm centers via μ_2-$\eta^1 : \eta^1$ coordination. The 2,7-nds also adopts one binding mode with each 2,7-nds coordinating to only two Sm centers via $\mu^1\eta^1$–$\mu^1\eta^1$ bridging, and leaving four free oxygens. In view of this connection mode of ina and the affinity of lanthanide ions for oxygen donors, two Sm(III) centers, Sm1 and Sm1A (A = symmetry code: $1 + x$, $-1 + y$, $-z$), are bridged by bidentate carboxyl groups of ina ligands to construct a dinuclear subunit $[Sm_2(ina)_4]$ with a Sm···Sm distance of 4.549 Å which is longer than the Ln(III)–Ln(III) distances of 4.401(2)–4.4252(9) Å from paddle-wheel structures $[Ln_2(4\text{-cba})_6(phen)_2(H_2O)_2]$ (Ln = Pr, Nd, Sm, Eu, Gd and Dy; 4-Hcba = 4-cyanobenzoicm acid; phen = 1,10-phenanthroline) [36], perhaps because the chelating coordination mode of phen ligands make the distances of Ln···Ln shorter. However, the most important aspect is that this arrangement provides active nitrogens with affinity of Cu(II) ions to construct a 2-D 3d–4f heterometallic network, which can be considered as a (4,4) net, as shown in figure 2(a). The grid in the (4,4) net is 8.956 Å × 8.954 Å [figure 2(b)].

In the packing arrangement of 2-D layers, 2,7-nds plays an important role in connecting adjacent layers, forming a 3-D layer-pillared coordination polymer as illustrated in figure 3(c). To better understand how 2,7-nds ligands link 2-D layers to 3-D framework, each 2,7-nds ligand bridges two Sm_2O_8 cluster units from adjacent layers through two alternating

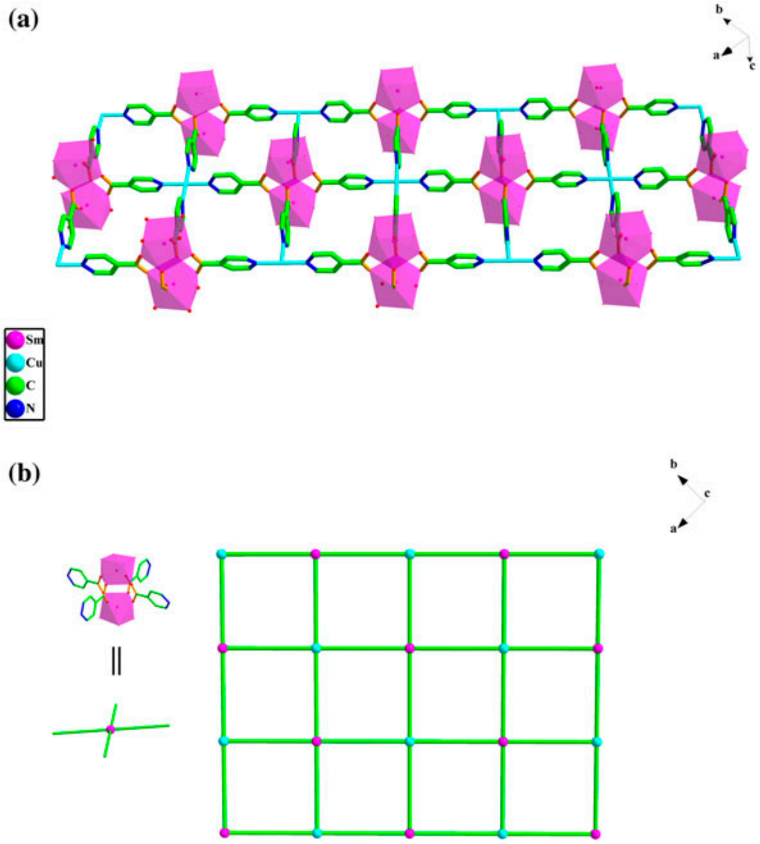

Figure 2. (a) A polyhedral view of the 2-D heterometallic layered network based on $[Sm_2(ina)_4]$ and Cu(II) in **2**. (b) View of the 2-D (4,4) net (8.956 Å × 8.954 Å). $[Sm_2(ina)_4]$ clusters are simplified to purple dots (see http://dx.doi.org/10.1080/00958972.2015.1027696 for color version).

fashions, one linking the upper square antiprisms of two Sm_2O_8 cluster units [figure 3(a)] and the other linking the lower square antiprisms of two Sm_2O_8 cluster units [figure 3(b)]. Detailed analyses reveal that **1–4** are chiral networks. Chirality comes from coordination of the nds groups and the configuration of metal geometry [52]. For example, the 3-D chiral network has all of its 2,7-nds ligands taking on rotational symmetry and all of its Ln centers displaying square-antiprism configurations [figure 3(a) and (b)], so that this structure layout gives chirality. If the water molecules occupying the pore are removed, **1–4** have 348 $Å^3$ potential solvent volume (6.4%) for **1**, 310 $Å^3$ potential solvent volume (5.9%) for **2**, 302 $Å^3$ potential solvent volume (5.6%) for **3**, and 290 $Å^3$ potential solvent volume (5.4%) for **4** estimated by PLATON [36]. Probably, 2,7-nds ligands occupy the channels when they coordinate at both sides of Ln_2 paddle-wheel units, so that the accessible pore volume of **1–4** is very small.

3.2. *Infrared spectroscopy*

In IR spectra, all the complexes show similar bands; broad bands at 3100–3500 cm^{-1} may be assigned to ν(O–H) of water molecules. The features at 1660–1558 cm^{-1} and

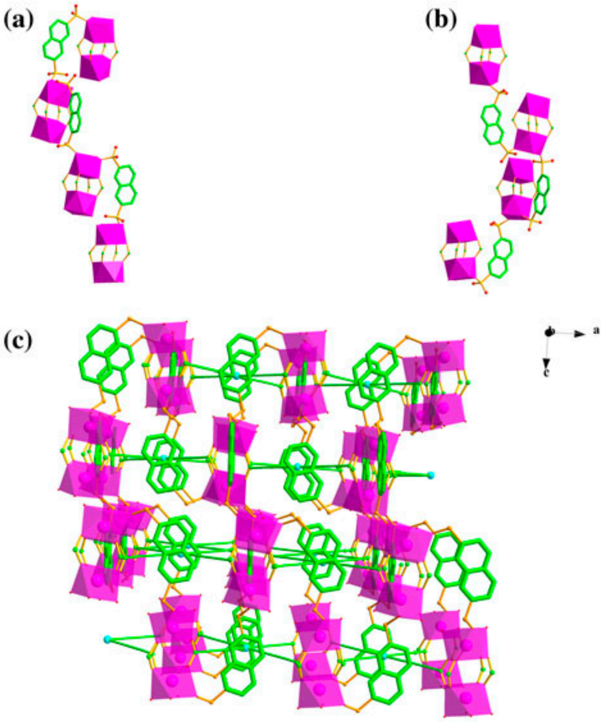

Figure 3. (a) The 2,7-nds ligand linking the upper square antiprisms of two Sm_2O_8 cluster units. (b) The 2,7-nds ligand linking the lower square antiprisms of two Sm_2O_8 cluster units. (c) View of the 3-D layer-pillared architecture constructed by 2,7-nds ligand bridging two Sm_2O_8 cluster units from the adjacent layers through upper–upper and lower–lower connections.

1401–1232 cm^{-1} are attributed to the ν_{asym}(C=O) and ν_{sym}(C=O) for carboxylate groups of Hina, respectively. There are no strong absorptions around 1700 cm^{-1}, suggesting that all of the carboxyl groups have been fully deprotonated in agreement with the results of the X-ray diffraction analysis. Band characteristics of ν_{asym}(S=O) and ν_{sym}(S=O) are observed at 1235–1171 cm^{-1} and 1120–1031 cm^{-1}, respectively [53].

3.3. *PXRD and thermal analysis results*

PXRD experiments were carried out for **1–4** at room temperature from $2\theta = 5 - 50°$. The patterns for the as-synthesized bulk materials closely match the simulated ones from the single-crystal structure analysis, which are indicative of pure solid-state phases (figure S1). To further determine the thermal stability of these compounds, **2** as a representative was investigated by TGA owing to the similarity of the structures for **1–4**. The TGA of **2** were done from 30 to 800 °C at a heating rate of 10 °C min^{-1} in dry air (figure 4). For **2**, a consecutive weight loss of the four lattice and four coordinated waters of 9.22% (Calcd 9.18%) was observed from 60 to 333 °C. After that, rapid weight loss observed above 350 °C is probably caused by decomposition of the 2,7-nds and ina ligands. Above 500 °C, the whole framework constructed by the 2,7-nds and ina ligands collapses 58.18% (Calcd 56.32%).

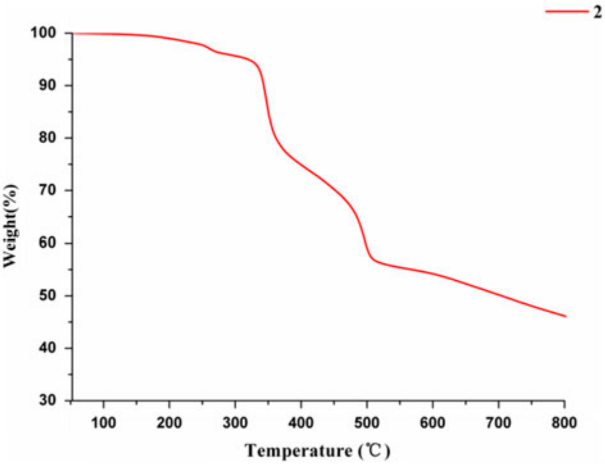

Figure 4. TG curve of **2**.

After the end of the experiment, we surmise the residue has a composition of 1.5 $Sm_2O_3\cdot$ 2CuO (found 46.06%; Calcd 47.36%).

3.4. *Photoluminescent properties*

Owing to the excellent luminescence of Nd(III), Sm(III), and Eu(III) ions, the photoluminescences of **1**, **2**, and **3** were investigated at room temperature. Complex **1** shows characteristic emission bands in the near-infrared region for Nd(III) ion when excited at 302 nm: three bands at 900(w), 1055(vs), and 1327(m) can be attributed to the $^4F_{3/2}$-$^4I_{9/2}$, $^4F_{3/2}$-$^4I_{11/2}$, and $^4F_{3/2}$-$^4I_{13/2}$, respectively (figure 5). However, **2** shows no characteristic emission spectra of Sm(III) and **3** exhibits no typical Eu(III) emissions. This may be attributed to the quenching

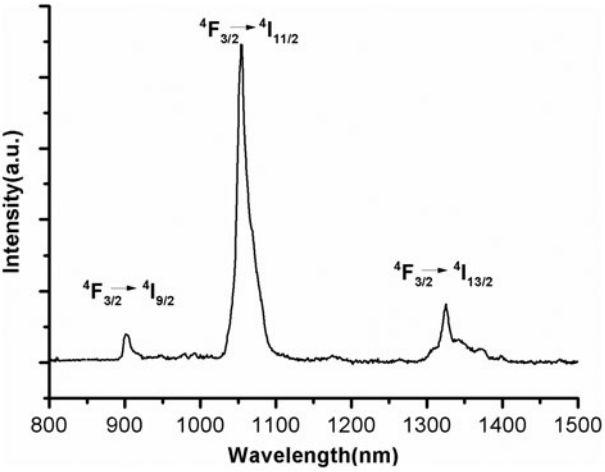

Figure 5. Solid-state emission of **1** at room temperature (ex = 302 nm).

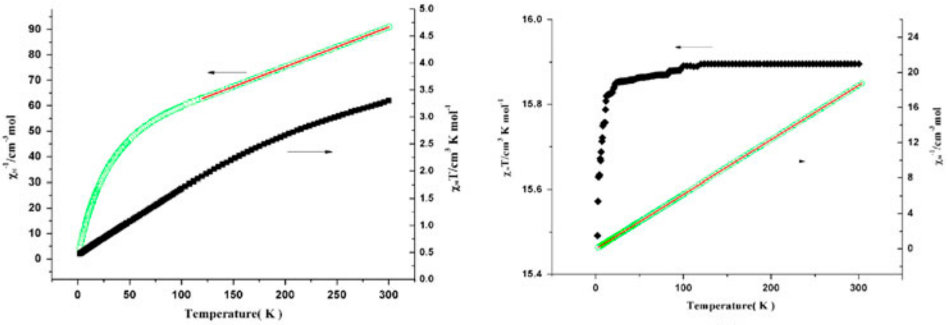

(a) **(b)**

Figure 6. (a) The $\chi_M T$ *vs.* T and $1/\chi_M$ *vs.* T curves for **3**. (b) The $\chi_M T$ *vs.* T and $1/\chi_M$ *vs.* T curves for **4**.

effect of high energy O–H vibrations of the water molecules in these complexes [54, 55]; another possibility is that the energy of the ligand-to-metal charge transfer state (LMCT state) is too low to sensitize Sm(III) and Eu(III) luminescence [56, 57], even though complexes contain d-block Cu(II) which can be used for sensitizing lanthanide luminescence [58, 59]. In fact, d-block metals are especially useful for sensitizing the near-infrared luminescence of lanthanide ions like Nd^{3+}, Er^{3+}, and Yb^{3+} [60], so that **1** has three emission bands in the near-infrared region.

3.5. *Magnetic properties*

Direct-current magnetic susceptibility studies were performed on microcrystalline samples of **3** and **4** at 1000 Oe from 2.0 to 300 K as plots of $\chi_M T$ *versus* T and $1/\chi_M$ *versus* T (figure 6). The $\chi_M T$ value of **3** is 3.30 cm^3 K mol^{-1} at 300 K, inconsistent with the calculated value for one spin-only Cu(II) (0.375 cm^3 K mol^{-1}, $S = 1/2$) and two ground-state Eu(III) (0 cm^3 K mol^{-1}, $^7F_0$) incorporated in one molecule. The disagreement may be ascribed to the presence of thermally populated exited states, as is well known for Eu(III) complexes [60, 61]. As shown in figure 6(a), the $\chi_M T$ value gradually decreases from 3.30 cm^3 K mol^{-1} to 0.47 cm^3 K mol^{-1} with the temperature decreasing from 300 to 2 K. The $1/\chi_M$ data above 119 K obey the Curie–Weiss law $\chi = C/(T - \theta)$ with $C = 6.39$ cm^3 K mol^{-1}, $\theta = -282.08$ K. The depopulation of the excited spin-orbit multiplets in the Eu(III) ion gives evidence of antiferromagnetic interactions existing in **3**. For **4**, as shown in figure 6(b), the value of $\chi_M T$ is 15.89 cm^3 K mol^{-1}, close to the spin-only value of 15.75 cm^3 K mol^{-1} for two Gd(III) ions ($S = 7/2$, $g = 2$). As the temperature decreases, the $\chi_M T$ value decreases gradually and reaches the minimum value of 15.49 cm^3 K mol^{-1} at 2 K. Curie–Weiss fitting of the magnetic data over the whole temperature range of 2–300 K results in a Curie constant $C = 15.85$ cm^3 K mol^{-1} and a Weiss constant $\theta = -0.213$ K, characteristic of an overall antiferromagnetic behavior by taking into account the fact that the orbital momentum of Gd(III) is completely quenched in the ground state [62, 63].

4. Conclusion

A new family of 3-D heterometallic 3d–4f coordination polymers, $[Ln_2Cu(2,7\text{-nds})_2(ina)_4(H_2O)_4]\cdot 4H_2O$ (Ln = Nd (**1**), Sm (**2**), Eu (**3**), Gd (**4**)), have been constructed by

2,7-naphthalenedisulfonate and isonicotinic acid under hydrothermal conditions. They are the first examples of Ln(III)–Cu(II) layer-pillared 3d–4f heterometallic compounds based on 2,7-nds, and a rare case that 2,7-nds ligands and ina–Cu–ina chains subtly connected two square antiprisms to build a 3-D structure in the family of Ln-TM heterometallic coordination polymers with organodisulfonate ligands. The syntheses of the title compounds provide a valuable approach for the construction of other heterometallic coordination polymers based on naphthalenedisulfonate ligands. Complex **1** exhibits a characteristic Nd(III)-centered luminescence, while **2** and **3** show no typical lanthanide-centered emissions for the quenching effect of highenergy O–H vibrations of the water molecules in them. The magnetic properties of **3** and **4** show antiferromagnetic behaviors.

Supplementary material

CCDC 969508-969511 contain the supplementary crystallographic data for **1–4**. These data can be obtained free of charge from the Cambridge Crystallographic Data Center via www.ccdc.cam.ac.uk/data_request/cif, or from the Cambridge Crystallographic Data Center, 12 Union Road, Cambridge CB2 1EZ, UK [Fax: +44 (1223) 336–033; E-mail: deposit@ccdc.cam.ac.uk].

Disclosure statement

No potential conflict of interest was reported by the authors.

Funding

This work was financially supported by the National Nature Science Foundation of China [grant number 20971047], [grant number U0734005], [grant number 21271076]; Key Program of Guangdong Universities Science and Technology innovation [grant number cxzd1020]; the Planning Program of Guangzhou City Science and Technology [grant number 2013J4100049].

References

[1] D.S. Reddy, S. Duncan, G.K.H. Shimizu. *Angew. Chem. Int. Ed.*, **115**, 1398 (2003).
[2] F. Gándara, J. Perles, N. Snejko, M.A. Iglesias. *Angew. Chem. Int. Ed.*, **45**, 7998 (2006).
[3] T.Z. Forbes, S.C. Sevov. *Inorg. Chem.*, **48**, 6873 (2009).
[4] H. Wu, X.W. Dong, H.Y. Liu, J. Yang, Y.Y. Liu, Z.M. Su. *Dalton Trans.*, **39**, 5331 (2008).
[5] W.J. Liu, N. Wang, Z.Q. Wei, X. Zhao, L.M. Chang, S.T. Yue, Y.L. Liu, Y.P. Cai. *Inorg. Chem. Commun.*, **14**, 1807 (2011).
[6] Y.Q. Sun, Q. Liu, J.C. Zhong, Q.F. Pan, Y.P. Chen. *J. Solid State Chem.*, **206**, 85 (2013).
[7] F. Gándara, A. García-Cortés, M. Iglesias, N. Snejko. *Inorg. Chem.*, **46**, 3475 (2007).
[8] B.D. Chandler, D.T. Cramb, G.K.H. Shimizu. *J. Am. Chem. Soc.*, **128**, 10403 (2006).
[9] P. Kanoo, K.L. Gurunatha, T.K. Maji. *Cryst. Growth Des.*, **9**, 4147 (2009).
[10] X. Ribas, D. Maspoch, K. Wurst, J. Veciana, C. Rovira. *Inorg. Chem.*, **45**, 5383 (2006).
[11] B.D. Chandler, J.O. Yu, D.T. Cramb, G.K.H. Shimizu. *Chem. Mater.*, **19**, 4467 (2007).
[12] S. Hu, K.H. He, M.H. Zeng, H.H. Zou, Y.M. Jiang. *Inorg. Chem.*, **47**, 5218 (2008).
[13] J.W. Cai. *Coord. Chem. Rev.*, **248**, 1061 (2004).
[14] J.P. Zhao, B.W. Hu, F.C. Liu, X. Hu, X.H. Bu. *CrystEngComm*, **9**, 902 (2007).
[15] X.P. Ye, W.J. Liu, N. Wang, S.T. Yue. *J. Coord. Chem.*, **66**, 191 (2013).
[16] J.L. Nicholls, S.E. Hulse, M.B. Hursthouse, A.M. Fogg. *Inorg. Chem.*, **49**, 8545 (2010).
[17] W.J. Liu, Z.Y. Li, N. Wang, X.X. Li, Z.Q. Wei, S.T. Yue, Y.L. Liu. *CrystEngComm*, **13**, 138 (2011).

[18] W.P. Xie, N. Wang, Y. Long, X.R. Ran, J.Y. Gao, C.J. Chen, S.T. Yue, Y.P. Cai. *Inorg. Chem. Commun.*, **40**, 151 (2014).
[19] F.C. Liu, Y.F. Zeng, J. Jiao, X.H. Bu, J. Ribas, S.R. Batten. *Inorg. Chem.*, **45**, 6129 (2006).
[20] T. Kurc, J. Janczak, J. Hoffmann, V.V. Adrabinska. *Cryst. Growth Des.*, **12**, 2613 (2012).
[21] Y.F. Zhou, M.C. Hong, X.T. Wu. *Chem. Commun.*, **2**, 135 (2006).
[22] C.J. Chen, N. Wang, W.P. Xie, X.R. Ran, S.T. Yue. *CrystEngComm*, **15**, 4611 (2013).
[23] M.D. Ward. *Coord. Chem. Rev.*, **251**, 1663 (2007).
[24] L. Liang, G. Peng, L. Ma, H. Deng, H. Li, W.S. Li. *Cryst. Growth Des.*, **12**, 1151 (2012).
[25] Y. Wang, P. Cheng, J. Chen, D.Z. Liao, S.P. Yan. *Inorg. Chem.*, **46**, 4530 (2007).
[26] C.J. Li, Z.J. Lin, M.X. Peng, M.M. Yang, M.L. Tong. *Chem. Commun*, **47**, 6348 (2008).
[27] M. Shibasaki, N. Yoshikawa. *Chem. Rev.*, **102**, 2187 (2002).
[28] V. Chandrasekhar, A. Chakraborty, E.C. Sañudo. *Dalton Trans.*, **42**, 13436 (2013).
[29] A.J. Shubnell, E.J. Kosnic, P.J. Squattrito. *Inorg. Chim. Acta*, **216**, 101 (1994).
[30] G.K.H. Shimizu. *Coord. Chem. Rev.*, **245**, 49 (2003).
[31] G.K.H. Shimizu, R. Vaidhyanathan, J.M. Taylor. *Chem. Soc. Rev.*, **38**, 1430 (2009).
[32] R.G. Pearson. *J. Am. Chem. Soc.*, **85**, 3533 (1963).
[33] Y.K. He, H.Y. An, Z.B. Han. *Solid State Sci.*, **11**, 49 (2009).
[34] R.H. Zeng, G. Peng, W.S. Li, Y.P. Cai. *CrystEngComm*, **13**, 3910 (2011).
[35] S. Gao, S.W. Ng. *Acta Crystallogr. Sect. E*, **67**, 1787 (2011).
[36] Y. Li, J.S. Huang. *Inorg. Chem.*, **45**, 6398 (2006).
[37] G.S. Guo, H.Y. Guo. *J. Rare Earths*, **26**, 633 (2008).
[38] G.M. Sheldrick. *SHELXL-97, Program for Crystal Structure Solution*, University of Göttingen, Göttingen, Germany (1997).
[39] G.M. Sheldrick. *SHELXL-97, Program for Crystal Structure Refinement*, University of Göttingen, Göttingen, Germany (1997).
[40] J.Y. Liu, N. Ren, J.J. Zhang, S.M. He, S.P. Wang. *Ind. Eng. Chem. Res.*, **52**, 6156 (2013).
[41] B.J. Gunderman, I.D. Kabell, S.N. Dubey. *Inorg. Chim. Acta*, **258**, 237 (1997).
[42] J.W. Cai, J.S. Zhou, M.L. Lin. *J. Mater. Chem.*, **13**, 1806 (2003).
[43] C.J. Chen, J.Y. Gao, W.P. Xie, X.R. Ran, S.T. Yue. *CrystEngComm*, **15**, 4611 (2013).
[44] F.H.Allen, O.Kennard, D.G.Watson. *J. Chem. Soc., Perkin Trans. II*, **12**, S1 (1987).
[45] A.J. Bondi. *Phys. Chem.*, **68**, 441 (1964).
[46] Z.Y. Li, N. Wang, S.T. Yue. *CrystEngComm*, **11**, 2003 (2009).
[47] Y.Z. Ma, L.M. Zhang, G. Peng, C.J. Zhao, R.T. Dong, C.F. Yang, H. Deng. *CrystEngComm*, **16**, 667 (2014).
[48] W. Haberditzl. *Angew. Chem. Int. Ed.*, **5**, 288 (1966).
[49] E.C. Yang, X.G. Wang, C.H. Zhang, N. Yang, Z.Y. Liu, X.J. Zhao. *Sci. Chin. Chem.*, **56**, 465 (2013).
[50] J.X. Liu, Y.F. Hu, R.L. Lin, S.F. Xue, Q.J. Zhu, T. Zhu. *CrystEngComm*, **14**, 6983 (2012).
[51] X. Zhao, D.X. Wang, G.Y. Lin, S.T. Yue, Y.P. Cai. *Inorg. Chem. Commun.*, **23**, 127 (2012).
[52] S.L. Cai, W.G. Zhang. *Cryst. Growth Des.*, **12**, 2355 (2012).
[53] Q.Y. Liu, W.F. Wang, Y.L. Wang, M.S. Wang, J.K. Tang. *Inorg. Chem.*, **51**, 2381 (2012).
[54] M.D. Allendorf, C.A. Bauer, R.K. Bhakta, R.J.T. Houk. *Chem. Soc. Rev.*, **38**, 1330 (2009).
[55] Y.J. Cui, Y.F. Yue, G.D. Qian, B.L. Chen. *Chem. Rev.*, **112**, 1126 (2012).
[56] W.H. Fonger, C.W. Struck. *J. Chem. Phys.*, **52**, 6364 (1970).
[57] K. Binnemans. *Chem. Rev.*, **109**, 4283 (2009).
[58] D. Imbert, M. Cantuel, G. Bernardinelli, C. Piguet. *J. Am. Chem. Soc.*, **125**, 15698 (2003).
[59] M.D. Ward. *Coord. Chem. Rev.*, **251**, 1663 (2007).
[60] N.M. Shavaleev, G. Accorsi. *Inorg. Chem.*, **44**, 61 (2005).
[61] T. Kido, Y. Ikuta, Y. Sunatsuki, Y. Ogawa, N. Matsumoto. *Inorg. Chem.*, **42**, 2 (2003).
[62] Y.P. Cai, Q.Y. Yu, Z.Y. Zhou, N. Wang, L. Chen, C.Y. Su. *CrystEngComm*, **11**, 1006 (2009).
[63] C. Benelli, D. Gatteschi. *Chem. Rev.*, **102**, 2369 (2002).